Finite-Element Modeling and Control of Flexible Fabric Parts

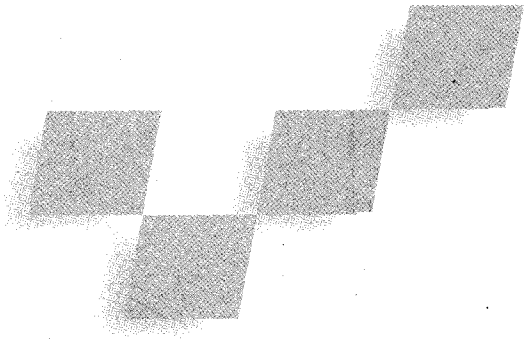

Jeffrey W. Eischen, Shigan Deng, and Timothy G. Clapp
North Carolina State University

The automotive and aircraft industries (among many others) have streamlined their design and manufacturing processes by adopting CAD/CAM approaches. The textile and apparel industries, however, have only recently acquired the proper physical models and computational strategies to successfully simulate fabric drape and manipulation. As these fundamental concepts become more sophisticated, the textile and apparel industries can adapt CAD/CAM processes to their own manufacturing and design processes, thereby increasing their competitiveness by increasing flexibility and quality and decreasing response times.

Accordingly, textile and apparel manufacturers are looking to automate facilities in their conventional production lines. In fabric assembly, they are considering automation for fabric pick-up and lay-down, fabric draping on the stacker, and intermediate operations such as fabric folding. Designers of fabric products also look to benefit from simulation capabilities that address variable material properties (weight, stiffness, and so on).

In this article, we describe simulation software that fulfills these manufacturing and design requirements. The software is based on stress-resultant, geometrically exact, nonlinear shell theory. It addresses nonlinear material response, fabric contact with rigid surfaces, and adaptive arc-length control. It can simulate 3D motions related to real fabric-manufacturing processes. We expect these capabilities to advance the technologies necessary to automate the textile and apparel industries.

Software based on nonlinear shell theory can simulate 3D motions related to real fabric-manufacturing processes. This simulation capability advances the technologies necessary for automating the textile and apparel industries.

Literature review

The state of the art in fabric drape simulation can be traced to the work of Peirce,[1] who in 1930 initiated research in the bending behavior of fabric and the measurement of its material properties. Peirce measured fabric flexural rigidity using a simple cantilever test and also modeled a typical woven fabric. In 1951, Abbott[2] reported using five different experimental methods to measure flexural rigidity. He also presented clustering and rigidity factors on fabric flexural rigidity. Cooper[3] later measured flexural rigidity of fibers, yarns and woven fabrics using the cantilever test.

After 1960, the study of fabric mechanics concentrated on fabric-buckling behavior. Dahlberg[4] modeled fabrics as thin plates and analyzed them with Euler's column-buckling formulation. He also conducted buckling tests to obtain load-deflection curves for fabrics. Lindberg, Behre, and Dahlberg[5] analyzed various commercial fabrics to obtain load-deformation curves for shearing and also to define plate- and shell-buckling behavior. Grosberg and Swani[6] described fabric bending behavior in terms of a bending-rigidity factor and an internal frictional couple.

Konopasek and Hearle[7] formulated a 3D fabric bending model that handled large deformations. They used moment-curvature equations, moment and force equilibrium equations, curvature-orientation equations, and orientation-coordinate equations to describe the fabric-bending curve, and the fourth-order Runge-Kutta method to numerically integrate a large set of nonlinear differential equations. Shanahan, Lloyd and Hearle[8] used small-deformation linear-plate and shell theory to characterize the mechanical behavior of fabric in complex deformations. Lloyd, Shanahan and Konopasek[9] studied the folding of heavy fabric sheets.

Lloyd[10] successfully applied a finite-element method to the analysis of complex fabric deformations. However, he treated only in-plane deformations and neglected bending, twisting deformations, and transverse shear-strain fields. Norton[11] modeled fabrics as 2D anisotropic elastic continua using differential geometry to develop the theory of fabric deformation as a Lagrangian field theory. However, he did not present a computational scheme for solving the nonlinear field equations.

Amirbayat and Hearle[12] described fabric buckling through minimization of the energy of deformation.

0272-17-16/96/$5.00 © 1996 IEEE

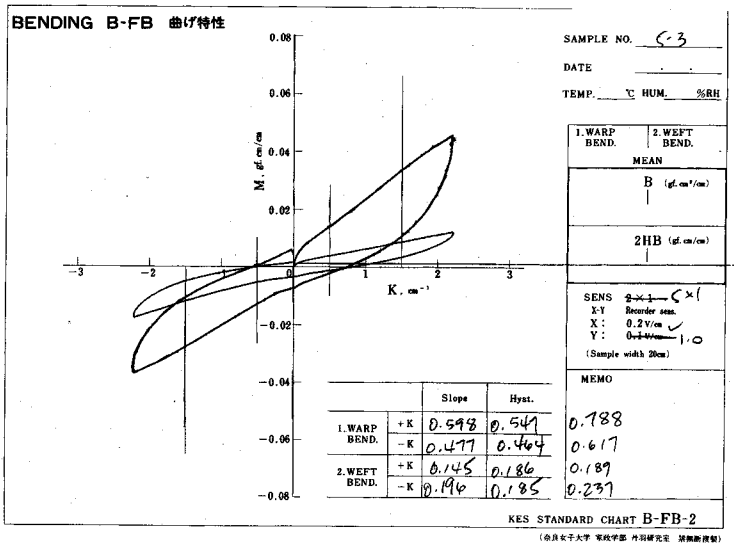

1 Output from Kawabata bending test.

They presented numerical solutions to isotropic Hookean materials. Brown, Buchanan, and Clapp[13] investigated the large bending deformation of fabrics in automated material handling, especially for laying out a fabric on a flat work surface. They developed a computer program based on Konopasek's theoretical formulation.

Clapp and Peng[14,15] investigated the effect of self-weight on the buckling behavior of fabrics under three different boundary conditions numerically using Timoshenko's elastica beam theory. They demonstrated the important role of fabric weight in buckling behavior.

Recently, there has been increased interest in true 3D modeling and analysis of fabric drape. Imaoka et al.[16] modeled fabrics using rod elements and bending springs. They carried out simulations of the draping of skirt shapes. Izumi and Niwa[17] studied the dynamic drape of ladies dress fabrics and correlated the results with mechanical properties such as bending rigidity and self-weight. Weil[18] produced 3D drape images by modeling the fabric as a constrained system of grid points. Material properties did not enter the analysis. Terzopoulos et al.[19] analyzed 3D deformable surfaces using nonlinear elasticity theory with a simplified stress-strain response. The stress-strain response did not employ standard engineering measures of rigidity like Young's modulus.

Von Der Weeën[20] developed algorithms for draping biaxially woven fabrics on a double-curved surface. He modeled fabrics as two families of perpendicular inter-locked inextensible fabrics. Gan et al.[21,22] developed a finite-element method to treat 3D drape based on shell/plate theory. They treated both linear and nonlinear moment curvature relationships, with different responses in the warp and weft directions. They considered membrane response to be nonlinear and presented simulations of sheets draping over square and circles.

Kim[23] showed how to treat 3D drape using the geometrically exact shell theory proposed by Simo et al.[24-26] Kim's method consistently accounts for all engineering properties such as modulus, weight, and thickness. Collier et al.[27] used orthotropic shell theory to treat draping behavior, including the effect of geometric nonlinearity. The drape of an annular shape was studied in detail. Breen et al.[28] developed a particle model for cloth with mechanical constraints to represent thread interactions.

Deng[29] extended the work of Kim[23] to treat buckling, nonlinear bending, and contact. This approach models the fabric as a 3D (shell) continuum. Kang and Wu[30] also used a continuum model (plate) for fabric drape, allowing for different mechanical response properties in the warp and weft directions. They showed the drape response of circular parts over circular pedestals and rectangular parts over rectangular pedestals. Chen and Govindaraj[31] presented further results on 3D drape using a degenerated solid-shell theory. Their results included square fabric parts draping over a flat square surface.

The work presented here is closely related to previous work using nonlinear continuum shell theory. A key extension is the ability to treat manipulation problems, specifically, situations where a drape shape continually changes because a point or points on the fabric have some specified motion. We begin by describing the assumed fabric material response and the physical modeling of fabric via nonlinear shell theory (mathematical details of the theory are included in an appendix on *IEEE CG&A*'s Web site).

Fabric material response

Fabrics generally show nonlinear response in bending. Their nonlinear moment-curvature response is often measured by the Kawabata Bending Test System.[32] One fabric used in this study was a twill-weave, 100-percent cotton fabric. It had the following physical properties:

- thickness, $h = 0.0489$ cm
- cross-sectional area, $A = 0.0489$ cm^2
- second moment of area, $I = 9.744 \times 10^{-6}$ cm^4
- weight density, $\omega = 0.02665$ gmf/cm^2

where gmf/cm^2 is grams-force per centimeter squared.

We used a 1-cm-wide strip to make all measurements. The moment-curvature for the cotton fabric was plotted automatically on a Kawabata Bending Tester, as shown in Figure 1. The simulations used the "*B*" value

On the Web: Details of nonlinear shell theory

Readers interested in nonlinear shell theory will find details in an appendix to this article on *CG&A*'s Web site: http://www.computer.org/pubs/cg&a/cg&a.html. The appendix includes a kinematic description of the shell, momentum balance equations, constitutive equations, and the static weak form of the equilibrium equations.

for positive curvature ($+K$) in the warp direction as the effective linear bending rigidity, $(EI)_{eff}$, which equaled 0.589 gmf – cm^2/cm. (B value is generated automatically by the Kawabata Test system.) We obtained a nonlinear moment-curvature response by fitting the actual measured $M - K$ curve with a fifth-order polynomial, according to the graph in Figure 2. Thus,

$$M = 1.33387K - 2.23070K^2 + 2.36510K^3 - 1.08471K^4 + 0.17876K^5$$

In this equation, K is the curvature with unit cm^{-1} while M is the moment per unit length with units gmf – cm/cm.

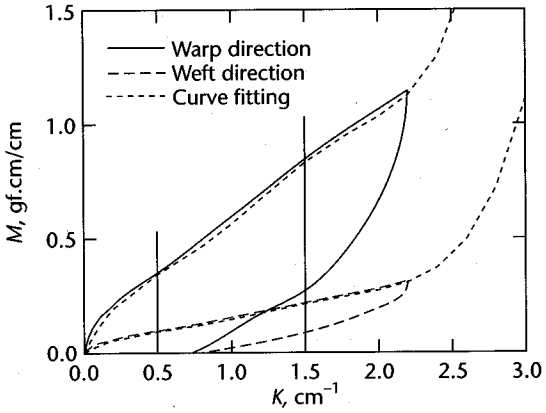

2 Curve fitting for output from Kawabata bending test.

Physical modeling of the fabric

Our software uses a physical model based on the geometrically exact shell theory conceived by Simo et al.[24-26] We briefly review our formulation of this model here. For complete details, see Deng.[29]

The kinematic description of the shell starts by parameterizing the position of points within the shell, both on and off the midsurface. Referring to Figure 3, points off the midsurface are located by a position vector $\mathbf{\Phi}$,

$$\mathbf{\Phi}(\xi^1,\xi^2,\xi) = \boldsymbol{\phi}(\xi^1,\xi^2) + \xi\mathbf{t}(\xi^1,\xi^2)$$

where $\boldsymbol{\phi}$ is a position vector locating points on the shell's midsurface (reference surface). The vector $\mathbf{t}$ is called the *director*; it is a unit vector directed along shell fibers that are initially perpendicular to the reference surface. The coordinate ξ measures distance between the midsurface and points off the midsurface along $\mathbf{t}$. ξ^1 and ξ^2 are dimensionless (non-arc-length) curvilinear coordinates. Note that the unit vector $\mathbf{t}$ is not necessarily normal to the midsurface of the deformed shell, thus admitting the possibility of transverse shear strain. The through-thickness coordinate ξ is in the range $-h/2 \le \xi \le h/2$, where h is the shell thickness. The undeformed configuration of the shell is given by

$$\mathbf{\Phi}_0(\xi^1,\xi^2,\xi) = \boldsymbol{\phi}_0(\xi^1,\xi^2) + \xi\mathbf{t}_0(\xi^1,\xi^2)$$

where $\boldsymbol{\phi}_0$ is a vector locating points on the undeformed midsurface and $\mathbf{t}_0$ is the director in the initial configuration, assumed normal to the midsurface. The essential problem is to determine the evolution of $\boldsymbol{\phi}$ and $\mathbf{t}$ as the shell deforms under its own weight or is manipulated in some way.

The evolution of the unit director vectors $\mathbf{t}(\xi^1,\xi^2)$ during a motion of the shell depends on an orthogonal transformation matrix $\mathbf{\Lambda}$. Let $\mathbf{t} = \mathbf{\Lambda E}$, where $\mathbf{\Lambda}$ is an orthogonal matrix such that $\mathbf{\Lambda\Lambda}^T = \mathbf{I}$ and $\mathbf{E}$ is an inertially fixed unit vector. Thus, to determine $\mathbf{t}$ during the shell motion, it is sufficient (or equivalent) to determine the matrix $\mathbf{\Lambda}$. At any point on the shell, this matrix is related to the unit director vector according to

$$\mathbf{\Lambda} = (\mathbf{E}\cdot\mathbf{t})\mathbf{I} + \widehat{\mathbf{E}\times\mathbf{t}} + \frac{1}{1+\mathbf{E}\cdot\mathbf{t}}(\mathbf{E}\times\mathbf{t})\otimes(\mathbf{E}\times\mathbf{t})$$

where $\hat{}$ indicates the skew symmetric matrix associated with the indicated vectors and $\otimes$ represents a tensor outer product operator.

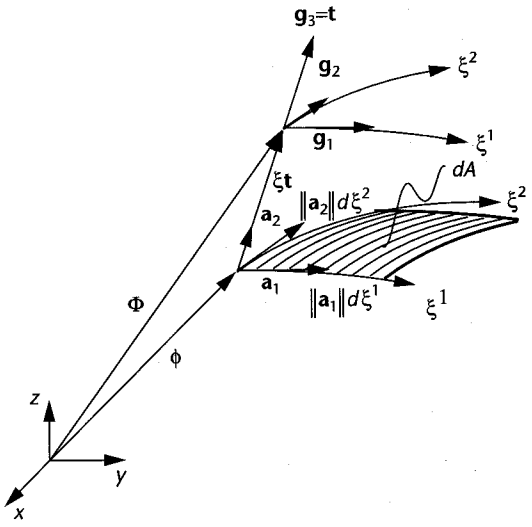

3 Configuration of the shell.

Enforcing linear and angular momentum allows development of a weak (or variational) form of the nonlinear shell theory. After incorporating the fabric material response, standard finite-element linearization procedures lead to a matrix equation of the form

$$\mathbf{K}(\boldsymbol{\phi},\mathbf{t})\begin{Bmatrix}\Delta\boldsymbol{\phi}\\ \Delta\mathbf{t}\end{Bmatrix} = \mathbf{F}_{ext} - \mathbf{P}(\boldsymbol{\phi},\mathbf{t}) \qquad (1)$$

where $\mathbf{K}(\boldsymbol{\phi},\mathbf{t})$ is the tangent stiffness matrix, $\mathbf{P}(\boldsymbol{\phi},\mathbf{t})$ is the internal force vector, and $\mathbf{F}_{ext}$ is the external force vector. Iterative solution of this matrix equation generates an incremental displacement vector $\Delta\boldsymbol{\phi}$, used to update the position of the shell midsurface, together with an incremental rotation matrix $\Delta\mathbf{\Lambda}$, used to update the directors as the shell deforms.

Specific algorithms

We used supplementary algorithms in conjunction with the basic finite-element method to deal with the unique problems of simulating fabric drape and manipulation. Arc-length control was necessary to account for buckling and a contact procedure was added to simulate fabric interactions with rigid objects.

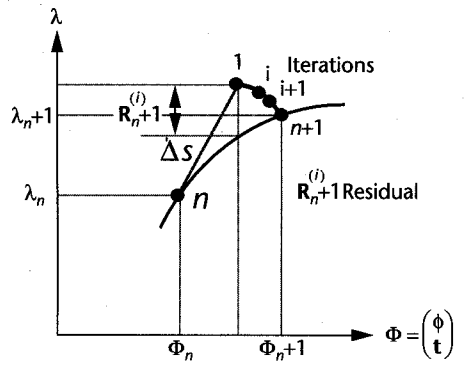

4 Load-displacement curve.

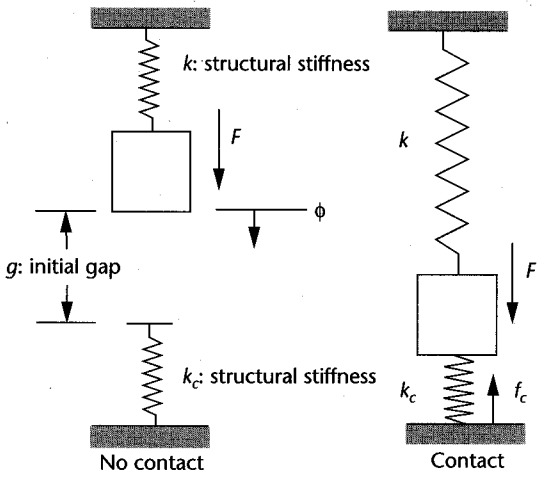

5 Contact treatment schematic.

Adaptive arc-length control algorithm

The finite-element equations (Equation 1) must be solved using a nonlinear iterative algorithm, such as Newton-Raphson. The basic Newton-Raphson algorithm fails when limit or bifurcation points are encountered along the load-deflection curve. The arc-length method of Schweizerhof and Wriggers[33] treats these cases by limiting the increments in force and/or displacement. We added an acceleration factor to their algorithm to allow a variable arc length based on the convergence behavior during previous load steps.

Based on numerical experiments, successful simulation of highly nonlinear structures, such as fabrics, depends heavily on the deformation during the first load step. Therefore, the initial load step (arc length) must be very small to avoid divergence. An excessive amount of computer time is expended in subsequent load steps if the initial arc length is held fixed. Therefore, after the first load step, the arc length can be enlarged to accelerate computational speed.

Referring to Figure 4, the finite-element equations (before linearization) for an equilibrium configuration at load step n are

$$\mathbf{P}(\mathbf{\Phi}_n, \lambda_n) - \mathbf{F}_{\text{ext}}(\lambda_n) = \mathbf{0}$$

where λ_n is a load factor defined by $\mathbf{F}_{\text{ext}} = \lambda \mathbf{F}_{\text{ref}}$ and $\mathbf{F}_{\text{ref}}$ is a reference external force (or displacment) vector.

The computational task is to advance the solution to a new equilibrium configuration $\mathbf{\Phi}_{n+1}$, λ_{n+1}. Note that $\mathbf{\Phi}_{n+1} = \mathbf{\Phi}_{n+1}(\phi_{n+1}, \mathbf{t}_{n+1})$. The arc-length method limits the excursion along the load-deflection curve by an amount Δs, as shown in Figure 4. The equilibrium equations must be satisfied at load step at $n + 1$,

$$\mathbf{P}(\mathbf{\Phi}_{n+1}, \lambda_{n+1}) - \mathbf{F}(\lambda_{n+1}) = \mathbf{0}$$

Schweizerhof and Wriggers[33] introduced a constraint equation

$$f = \left[(\mathbf{\Phi}^i_{n+1} - \mathbf{\Phi}_n)\cdot(\mathbf{\Phi}^i_{n+1} - \mathbf{\Phi}_n) + (\lambda^i_{n+1} - \lambda_n)^2\right]^{1/2} - \gamma_n \Delta s = 0$$

where Δs is the arc-length control constant, γ_n is the newly introduced acceleration factor, and i is the algorithm iteration counter. The acceleration factor γ_n can be defined as a constant or any function. Here we define it as

$$\gamma_n \equiv \begin{cases} 1 & \text{for } n = 1 \\ N_p / N_{n-1} & \text{for } n > 1 \end{cases}$$

where N_p is the target number of iterations per load step and N_{n-1} is the actual number of iterations for the last load step.

If γ_n is set to 1 for all time, then the constraint reverts to the form of Schweizerhof and Wriggers. Upon linearizing both the equilibrium and the constraint equations, we obtain the following equations:

$$\Delta\lambda^i_{n+1} = -\frac{f^i(f^i + \gamma_n \Delta s) + (\mathbf{\Phi}^i_{n+1} - \mathbf{\Phi}_n)^T \Delta\mathbf{u}^{II}}{(\lambda^i_{n+1} - \lambda_n) + (\mathbf{\Phi}^i_{n+1} - \mathbf{\Phi}_n)^T \Delta\mathbf{u}^{I}}$$

where

$$\Delta\mathbf{\Phi}^i_{n+1} = \Delta\lambda^i_{n+1}\Delta\mathbf{u}^I + \Delta\mathbf{u}^{II}$$

$$\Delta\mathbf{u}^I \equiv \mathbf{K}^{i^{-1}}\mathbf{F}_0$$

$$\Delta\mathbf{u}^{II} \equiv \mathbf{K}^{i^{-1}}(\mathbf{F}^i_{ext} - \mathbf{P}^i)$$

$$\mathbf{K}^i = \left.\frac{\partial \mathbf{P}}{\partial \mathbf{\Phi}_{n+1}}\right|^i$$

$$\mathbf{F}_0 = \left.\frac{\partial \mathbf{F}}{\partial \lambda_{n+1}}\right|^i - \left.\frac{\partial \mathbf{P}}{\partial \lambda_{n+1}}\right|^i$$

Contact algorithm

We employed the penalty method indicated in Cook, Malkus, and Plesha[34] to treat fabric contact with rigid surfaces because it is simple to incorporate in finite-element analysis. Figure 5 shows a simple one-degree-of-freedom system that illustrates the essential features of the contact scheme. When the displacement ϕ is less than the initial gap g, the equilibrium equation is

$$P(\phi) = F$$

where $P(\phi) = k\phi$ is the internal elastic force and F is the

external force. Note that $\partial P/\partial\phi = k$. When $\phi > g$, equilibrium is achieved when

$$P(\phi) = F - F_c$$

where

$$P(\phi) = k\phi$$
$$F_c = k_c(\phi - g)$$

Upon linearization,

$$P(\phi) + \frac{\partial P}{\partial \phi}\Delta\phi + F_c(\phi) + \frac{\partial F_c}{\partial \phi}\Delta\phi = F$$

or

$$(k + k_c)\Delta\phi = F - P(\phi) - F_c(\phi)$$

Note that the incremental equilibrium equation used to solve for the displacement ϕ is

$$(k^i + k_c)\Delta\phi^i = F^i - P^i(\phi^i) - F_c^i(\phi^i)$$

where

$$F_c^i(\phi^i) = k_c(\phi^i - g)$$

The multidimensional analog of this simple example is then

$$[\mathbf{K}^i + \mathbf{K}_c^i]\Delta\mathbf{\Phi}_{n+1}^i = \mathbf{F}^i - \mathbf{P}^i - \mathbf{F}_c^i$$

where

$$\mathbf{K}_c = k_c \begin{bmatrix} 0 & 0 & 0 & 0 & \cdots & \cdots & 0 & 0 \\ & 1 & 0 & 0 & \cdots & \cdots & 0 & 0 \\ & & 1 & 0 & 0 & \cdots & 0 & 0 \\ \vdots & \vdots & \vdots & \vdots & \vdots & \vdots & \vdots & \vdots \\ & & & & & 0 & 0 & 0 \\ & & \textit{Sym.} & & & & 1 & 0 \\ & & & & & & & 0 \end{bmatrix}$$

$$\mathbf{F}_c = \begin{Bmatrix} F_c^1 \\ F_c^2 \\ \vdots \\ F_c^N \end{Bmatrix}, \quad F_c^I = \begin{cases} k_c(\phi^I - g^I) & \text{for a contact node} \\ 0 & \text{for no contact} \end{cases} \quad \textbf{(2)}$$

where contact at a particular node is indicated by a 1 in the corresponding diagonal entry in matrix $\mathbf{K}_c$, and k_c is the penalty constant. N is the total number of nodal points.

Note that the contact force F_c at node I is calculated according to Equation 2. ϕ^I is the current displacement at contact node I and g^I is the initial gap between node I and the contact surface.

Numerical simulations

We present several fabric drape and manipulation problems in this section. All simulations are based on four-node quadrilateral elements.

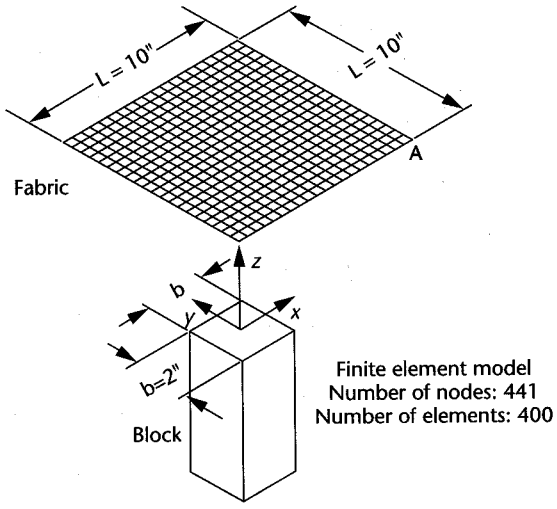

6 Finite-element model for a fabric draping over a block.

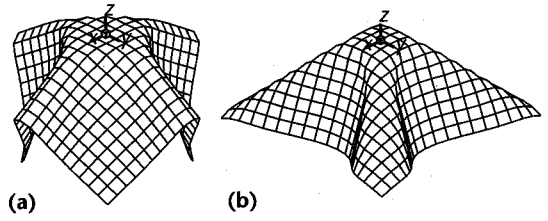

7 Deflection modes for fabric draping over a block: (a) large-deflection mode and (b) buckling mode.

Fabric draping over a block

In this simulation of fabric draping over a cubic block, the fabric is initially flat. Figure 6 shows the finite-element model. The physical properties and finite-element modeling assumptions are listed below:

- Physical properties
  - Material: polyester plain weave
  - Dimension (length × width × height): $10.0 \times 10.0 \times 0.02135$ inches
  - Effective Young's modulus: $E_{\text{eff}} = 2688$ oz/in^2
  - Weight density: $w = 5.425 \times 10^{-3}$ oz/in^2
- Finite element modeling assumptions
  - Linear elastic isotropic material properties
  - Fabric fixed at four corner points on the block (no contact algorithm)
  - Initially flat fabric sheet
  - Poisson's ratio: $v = 0.3$
  - Error tolerance for convergence:

$$\frac{\|\mathbf{R}^i\|}{\|\mathbf{R}^0\|} \le 1 \times 10^{-6}$$

We found two deformation modes during the numerical simulations, depending on the initial load-factor increment. The first deformation mode occurred for an initial load factor $\Delta\lambda_0 = 0.00025$. We call this the *large-deflection mode* (Figure 7a) because the deformation occurred smoothly without buckling, as indicated by the behavior of the convergence of the residual norm (Table 1). The second deformation mode occurred for

Table 1. Convergence rate of the residual norm during the first load step

Large-Deflection Mode		
Iteration Number	**Load Factor**	**Residual Norm**
1	2.50000000E-04	1.23640856E-02
2	5.20361759E-04	2.60812500E-05
3	4.76908770E-04	1.96680856E-04
4	4.76692968E-04	7.94723675E-07
5	4.76863579E-04	2.29410051E-09

Buckling Mode		
Iteration Number	**Load Factor**	**Residual Norm**
1	1.25000000E-03	5.32660728E-01
2	2.67446946E-02	7.75892434E-01
3	3.71447042E-02	1.38591371E-01
4	4.33657347E-02	9.70745612E-01
5	-4.50676735E-03	6.23254384E-02
6	6.89924664E-03	5.73646924E-02
7	9.95271217E-03	3.85140064E-02
8	9.46307718E-03	4.52604316E-02
9	9.13956848E-03	1.29163046E-02
10	8.12400477E-03	8.08075405E-03
11	8.05910433E-03	1.30888353E-04
12	8.05213315E-03	1.19106424E-06
13	8.05217588E-03	5.51333229E-11

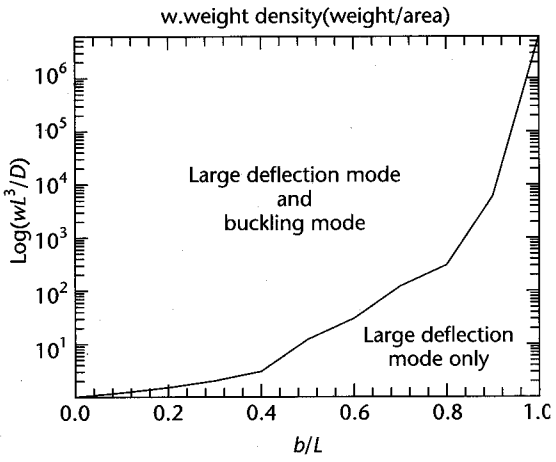

8 Effect of fabric bending rigidity and edge ratio *b/L*.

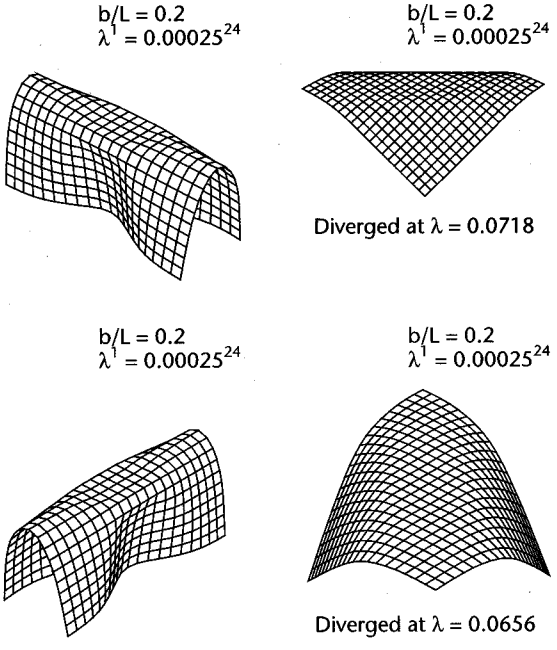

9 Four deflection modes for initially wavy fabric draping over a block.

$\Delta\lambda_0 = 0.00125$. We call this the *buckling mode* (Figure 7b) because the behavior of the residual norm in the first load step is erratic, indicating buckling (Table 1).

The particular drape shape encountered depends heavily on the bending rigidity $D = Eh^3/12(1-\nu^2)$ and the b/L ratio. Figure 8 shows the effect of these parameters on the buckling mode predicted by the simulation. Since the figure is plotted in dimensionless terms, it can be applied to any material once the shell's bending rigidity and b/L ratio are known. In this figure, the large-defection mode area can be also defined as the *stable area*. The *multiple solutions area* is characterized by the presence of both buckling and large-deflection modes. By locating the intersection point of D and b/L in Figure 8, it is easy to determine the stability of the draping condition.

Real fabrics contain geometric imperfections. We undertook a brief study of the effect of an initially wavy-surface (nonflat) fabric. The finite-element mesh was assigned a random waviness. A very slight waviness was allowed, whereby the z coordinate was restricted to the range $(-1 \times 10^{-4}$ in. $\le z \le 1 \times 10^{-4}$ in.). We repeated the simulation 20 times, each time with a different waviness pattern. All simulations used the same initial load factor of $\Delta\lambda_0 = 0.00025$. We discovered the four different drape modes shown in Figure 9. None of these is a buckling mode because the convergence of the residual norm was reached smoothly.

Fabric hanging over a round rod

We selected the cotton twill fabric described earlier (see "Fabric material response") to simulate a fabric hanging diagonally over a rod. The fabric's finite-element model was the same one used for draping over a block (see Figure 6), except the fabric dimension was 20×20 cm. A 2.5-cm radius rod supported the fabric, which was draped diagonally over the rod. The finite-element model assumed

- Elastic isotropic material for both linear and nonlinear material response.
- Fabric nodal points fixed along the diagonal line as a boundary condition.
- Contact algorithm applied for round rod.
- No contact friction.
- Initially flat fabric sheet.
- Poisson's ratio: $\nu = 0.3$.
- Target number of iterations: $N_p = 7$.
- Error tolerance for convergence:

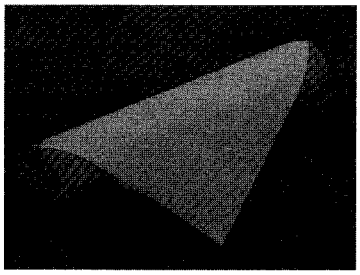

(a)

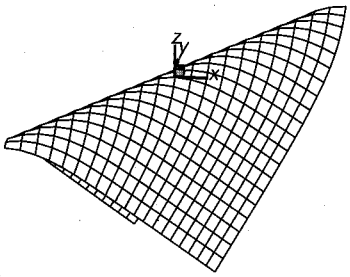

(b)

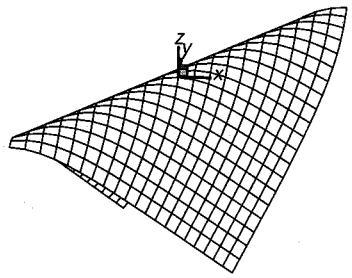

(c)

10 Fabric hanging over a round rod diagonally: (a) experimental result, (b) linear material solution, and (c) nonlinear material solution.

$$\frac{\|\mathbf{R}^i\|}{\|\mathbf{R}^0\|} \leq 1\times10^{-5}$$

Figure 10 shows the experimental result and a comparison of the linear and nonlinear material models. Table 2 shows the coordinates of corner point A (original coordinates: $x = 10$ cm, $y = -10$ cm, $z = 0.0$ cm) compared to the experimental result. It also lists the relative error between the numerical and experimental results.

Table 2. Comparison of corner node *A* coordinates for a fabric hanging over a rod diagonally.

Corner Node A	x (cm)	y (cm)	z (cm)	Error (percent)
Experimental result	3.47	−3.47	−12.25	–
Numerical solution (linear)	2.83	−2.83	−12.57	0.08
Numerical solution (nonlinear)	3.85	−3.85	−12.14	0.8

Folding a fabric strip

We simulated folding a fabric strip to test the efficiency of the adaptive arc-length control algorithm, using the Cray Y-MP supercomputer at the North Carolina Supercomputer Center (NCSC). Figure 11 shows the prescribed folding displacement. The material properties and finite-element modeling assumptions for this simulation are listed below:

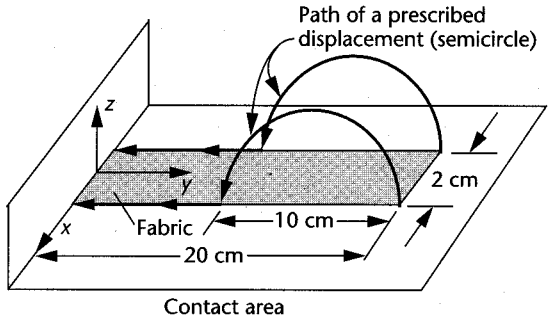

11 Prescribed displacement for fabric strip folding (efficiency study).

- Physical properties
  - Material: Polyester plain weave
  - Dimension: $20 \times 2 \times 0.0469$ cm
  - Young's modulus: $E = 4{,}196$ oz/in^2
  - Weight density: $w = 4.019 \times 10^{-3}$ oz/in^2
- Finite element modeling assumptions
  - Linear elastic isotropic material.
  - Contact algorithm applied.
  - No contact friction.
  - Three load/prescribed displacement regimes: self-weight load step (SW), prescribed semicircular displacement step (R), and prescribed translation displacement step (T).
  - 80×1 elements, 162 nodal points.
  - Poisson ratio: $v = 0.0$.
  - Error tolerance for convergence:

$$\frac{\|\mathbf{R}^i\|}{\|\mathbf{R}^0\|} \leq 1\times10^{-6}$$

Figure 12 shows the finite-element deformation sequence of this simulation. Table 3 shows the computational time and load steps with and without the acceleration factor. The acceleration factor increases computational efficiency by a factor greater than 10.

Fabric folding in 3D

Fabric folding is a common manipulation in the garment assembly process. We simulated 3D fabric folding, although limitations in computer speed prevented us from simulating a very fine finite-element model (that is, one consisting of many elements). Therefore, we performed a convergence study to define the relative error of different finite-element models. We also investigated the effect of linear versus nonlinear material response.

Convergence study for fabric folding. We used the strip geometry for the convergence study. Figure 13 (next page) shows a 20×1 cm fabric strip that we manipulated to follow a prescribed path (semicircle with 10-cm radius). The fabric material was again the twill-weave cotton described above. We included linear and nonlinear material responses and compared them with the experimental result. Three different finite-element meshes (20×1, 40×1, 80×1) were compared for final deformation with the experimental result. The finite-element model assumed

- Elastic isotropic material for both linear and nonlinear material response.
- Contact algorithm applied.

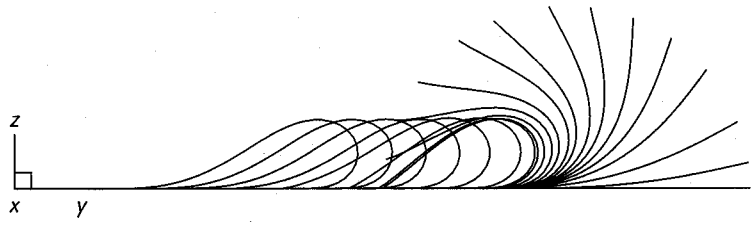

12 Deformation sequence for fabric folding.

- No contact friction.
- Two load/prescribed displacement regimes
  - Self-weight load step (SW).
  - Prescribed rotation displacement step (R).
- Target number of iterations: $N_p = 10$ for 20×1 and 80×1 models, and $N_p = 8$ for 40×1 model.
- Poisson ratio: $v = 0.0$ for excluding lateral effect.
- Error tolerance for convergence:

$$\frac{\|\mathbf{R}^i\|}{\|\mathbf{R}^0\|} \leq 1 \times 10^{-5}$$

Table 3. Efficiency comparison of adaptive arc-length control algorithm for $N_p = 10$.

	CPU Sec.	Load Steps	Initial arc-length $\Delta\lambda_0$ 1st (SW)	2nd (R)	3rd (T)
Without acceleration	1595.21	1994	2.70782672e-6	0.0009	0.001
With acceleration	121.48	45	2.70782672e-6	0.009	0.001

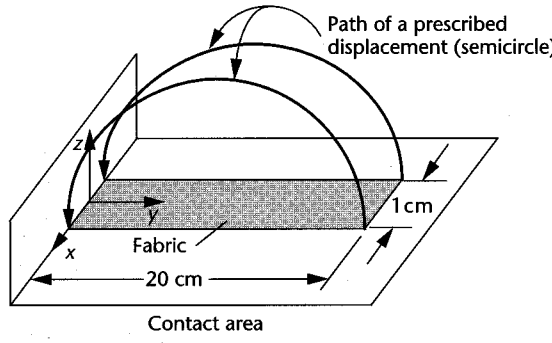

13 Prescribed displacement for fabric strip folding (convergence study).

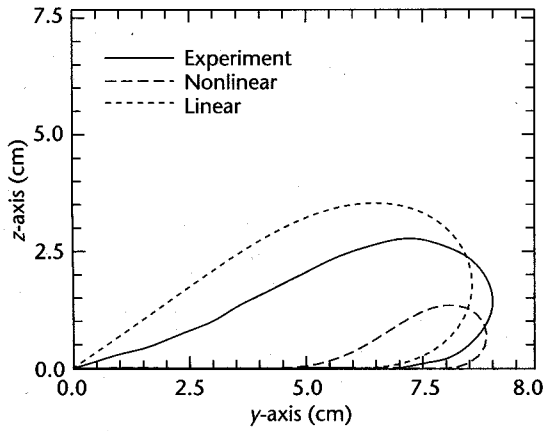

14 Final deflection shape comparison for fabric strip folding.

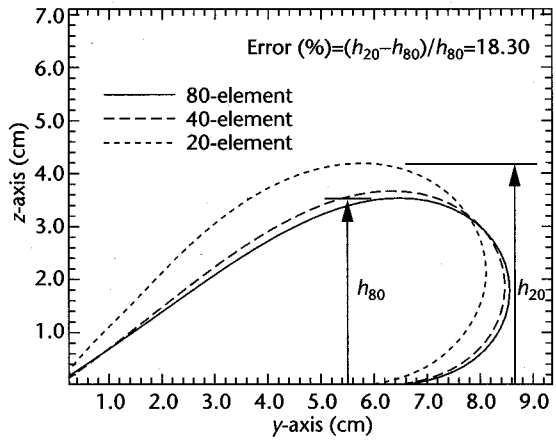

15 Convergence study for folding of fabric strip.

Figure 14 shows the numerical solutions for linear and nonlinear material responses and the experimental results. The finite-element mesh used for numerical solutions was 80×1. The figure shows that the nonlinear material model matched the experimental result better than the linear material model did.

Figure 15 shows the convergence study for final deformation shapes for 20-, 40-, and 80-element meshes. The results are essentially converged for 40 elements. Subsequent 3D folding simulation work will consider only nonlinear response. We think that fabric sheets modeled with 20 elements in each direction will be adequate, based on available computer resources. Since the relative error of loop height for 20 elements (h_{20}) and 80 elements (h_{80}) is around 18 percent for both materials, the final deformation for subsequent simulation should decrease by 18 percent of their loop height, if we consider the model with 80 elements on each side.

Square fabric folding on the diagonal. We simulated folding a 20×20 cm square fabric diagonally from one corner to the other. The folding path followed a semicircle with radius $r = 14.14$ cm. The finite-element model assumed:

- Elastic isotropic material for nonlinear material response.
- Contact algorithm applied for $z = 0$.
- No contact friction.
- Two load/prescribed displacement regimes:
  - Self-weight load step (SW).
  - Prescribed rotation displacement step (R), $r = 10\ cm$.
- 20×20 mesh, 441 nodal points.
- Poisson ratio $v = 0.3$
- Target number of iterations: $N_p = 7$.
- Error tolerance for convergence:

$$\frac{\|\mathbf{R}^i\|}{\|\mathbf{R}^0\|} \leq 1 \times 10^{-5}$$

Figures 16 and 17 show the step-by-step deformation comparison between the finite-element solutions and

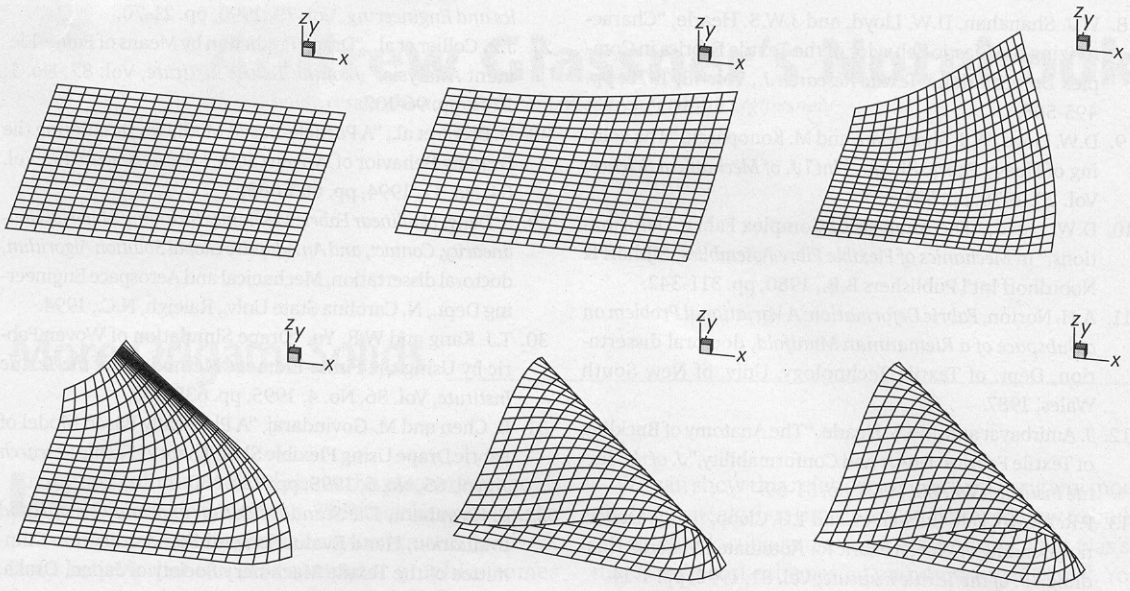

16 Fabric folding diagonally, numerical solution.

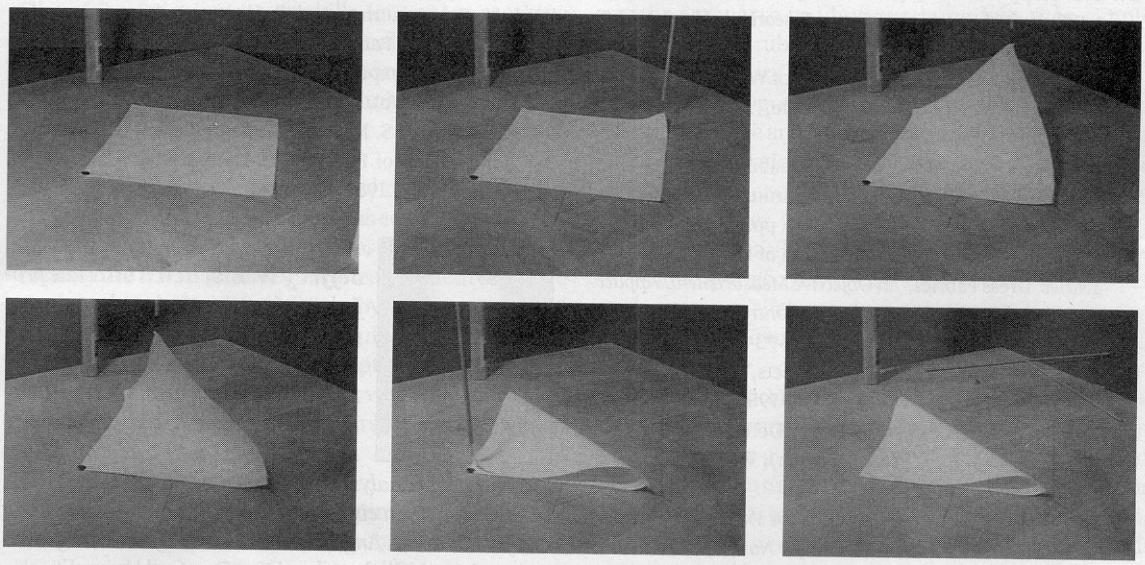

17 Fabric folding diagonally, experimental result.

the experimental results and the agreement between them. From the experience of fabric strip folding, the loop height of the final deformation shape should decrease 18 percent if the simulation used the model with 80 elements on each side. The numerical solution for 20 elements on each side is 4.22 cm in this case. It becomes 3.58 cm by reducing 18 percent. The loop height of the experimental result is 2.80 cm. Thus, the relative error between the experimental result and numerical simulation is 27.8 percent. Note the 3D deformations in the intermediate manipulation can be simulated and seen clearly.

Conclusions

The finite-element approach shows significant promise in the area of fabric motion simulation due to its inherent generality in dealing with arbitrary shapes, materials, loads, and contact surfaces. Future work must be directed at developing algorithms that promote faster solution times. Current solution times are excessive for use in complex "real-world" garments. ■

References

1. F.T. Peirce, "The Handle of Cloth as a Measurable Quantity," *J. of the Textile Institute*, Vol. 21, 1930, pp. T377-T416.
2. N.J. Abbott, "The Measurement of Stiffness in Textile Fabrics," *Textile Research J.*, Vol. 21, 1951, pp. 435-444.
3. D.N.E. Cooper, "The Stiffness of Woven Textile," *J. of the Textile Institute*, Vol. 51, 1960, pp. T317-T335.
4. B. Dahlberg, "Mechanical Properties of Textile Fabrics, Part II: Buckling," *Textile Research J.*, Vol. 31, 1961, pp. 94-99.
5. J. Lindberg and B. Dahlberg, "Mechanical Properties of Textile Fabrics, Part III: Shearing and Buckling of Various Commercial Fabrics," *Textile Research J.*, Vol. 31, 1961, pp. 99-122.
6. P. Grosberg and N.M. Swani, "The Mechanical Properties of Woven Fabrics," *Textile Research J.*, Vol. 36, 1966, pp. 338-345.
7. M. Konopasek and J.W.S. Hearle, "Computational Theory of Bending Curves. Part I: The Initial Value Problem for the Three-Dimensional Elastic Bending Curve," *Fibre Science and Technology*, Vol. 5, 1972, pp. 1-28.

8. W.J. Shanahan, D.W. Lloyd, and J.W.S. Hearle, "Characterizing the Elastic Behavior of the Textile Fabrics in Complex Deformation," *Textile Research J.*, Vol. 48, 1978, pp. 495-505.
9. D.W. Lloyd, W.J. Shanahan, and M. Konopasek, "The Folding of Heavy Fabric Sheets," *Int'l J. of Mechanical Science*, Vol. 20, 1978, pp. 521-527.
10. D.W. Lloyd, "The Analysis of Complex Fabric Deformations," in *Mechanics of Flexible Fibre Assemblies*, Sijthoff & Noordhoff Int'l Publishers B.B., 1980, pp. 311-342.
11. A.H. Norton, *Fabric Deformation: A Variational Problem on a Subspace of a Riemannian Manifold*, doctoral dissertation, Dept. of Textile Technology, Univ. of New South Wales, 1987.
12. J. Amirbayat and J.W.S. Hearle, "The Anatomy of Buckling of Textile Fabrics: Drape and Conformability," *J. of the Textile Institute*, Vol. 80, 1989, pp. 51-69.
13. P.R. Brown, D.R. Buchanan, and T.G. Clapp, "Large-Deflection Bending of Woven Fabric for Automated Material Handling," *J. of the Textile Institute*, Vol. 81, 1990, pp. 1-14.
14. T.G. Clapp and H. Peng, "Buckling of Woven Fabrics, Part I: Effect of Fabric Weight," *Textile Research J.*, Vol. 60, 1990, pp. 228-234.
15. T.G. Clapp and H. Peng, "Buckling of Woven Fabrics, Part II: Effect of Weight Frictional Couple," *Textile Research J.*, Vol. 60, 1990, pp. 285-292.
16. H. Imaoka et al., "Analysis of Drapeability by Computer," *Ann. Conf. Preprints*, Research Institute for Polymers and Textiles, Tsukuba City, Japan, 1981, pp. 1-9.
17. K. Izumi and W. Niwa, "Evaluation of Dynamic Drape of Ladies' Dress Fabrics," in *Objective Measurement: Applications to Product Design and Process Control*, Textile Machinery Society of Japan, 1985, pp. 725-734.
18. J. Weil, "The Analysis of Cloth Objects," *Computer Graphics* (Proc. Siggraph), Vol. 20, No. 4, 1986, pp. 49-53.
19. D. Terzopoulos et al., "Elastically Deformable Models," *Computer Graphics* (Proc. Siggraph), Vol. 20, No. 4, July 1987, pp. 205-214.
20. F. Von Der Weeën, "Algorithms for Draping Fabrics on Double-Curved Surfaces," *Int'l J. for Numerical Methods in Engineering*, Vol. 32, 1991, pp. 1415-1426.
21. L. Gan et al., "A Finite Element Analysis of the Draping of Fabrics," *Proc. 6th Int'l Conf. in Australia on Finite Element Methods*, 1991, pp. 402-414.
22. L. Gan et al., "A Study of Fabric Deformation Using Nonlinear Finite Elements," *Textile Research J.*, Vol. 65, No. 11, 1995, pp. 660-668.
23. J. Kim, *Fabric Mechanics Analysis Using Large Deformation Orthotropic Shell Theory*, doctoral dissertation, Mechanical and Aerospace Engineering Dept., North Carolina State Univ., Raleigh, N.C., 1991.
24. J.C. Simo and D.D. Fox, "On a Stress Resultant Geometrically Exact Shell Model. Part I: Formulation and Optimal Parameterization," *Computer Methods in Applied Mechanics and Engineering*, Vol. 72, 1989, pp. 267-304.
25. J.C. Simo, D.D. Fox, and M.S. Rifai, "On a Stress Resultant Geometrically Exact Shell Model. Part II: The Linear Theory; Computational Aspects," *Computer Methods in Applied Mechanics and Engineering*, Vol. 73, 1989, pp. 53-92.
26. J.C. Simo, D.D. Fox, and M.S. Rifai, "On a Stress Resultant Geometrically Exact Shell Model. Part III: Aspects of the Nonlinear Theory," *Computer Methods in Applied Mechanics and Engineering*, Vol. 79, 1990, pp. 21-70.
27. J.R. Collier et al., "Drape Prediction by Means of Finite-Element Analysis," *J. of the Textile Institute*, Vol. 82, No. 1, 1991, pp. 96-107.
28. D. Breen et al., "A Particle-Based Model for Simulating the Draping Behavior of Woven Cloth," *Textile Research J.*, Vol. 64, No. 11, 1994, pp. 663-685.
29. S. Deng, *Nonlinear Fabric Mechanics Including Material Nonlinearity, Contact, and An Adaptive Global Solution Algorithm*, doctoral dissertation, Mechanical and Aerospace Engineering Dept., N. Carolina State Univ., Raleigh, N.C., 1994.
30. T.J. Kang and W.R. Yu, "Drape Simulation of Woven Fabric by Using the Finite-Element Method," *J. of the Textile Institute*, Vol. 86, No. 4, 1995, pp. 635-648.
31. B. Chen and M. Govindaraj, "A Physically Based Model of Fabric Drape Using Flexible Shell Theory" *Textile Research J.*, Vol. 65, No. 6, 1995, pp. 324-330.
32. S. Kawabata, *The Standardization and Analysis of Hand Evaluation*, Hand Evaluation and Standardization Committee of the Textile Machinery Society of Japan, Osaka, Japan, 1975.
33. K.H. Schweizerhof and P. Wriggers, "Consistent Linearization of Path Following Methods in Nonlinear FE Analysis," *Computer Methods in Applied Mechanics and Engineering*, Vol. 72, 1986, pp. 267-304.
34. R.D. Cook, D.S. Malkus, and M.E. Plesha, Concepts and Applications of Finite Element Analysis, 3rd ed., John Wiley & Sons, 1989.

Jeffrey W. Eischen *is associate professor of mechanical and aerospace engineering at North Carolina State University. His research interests include linear and nonlinear finite-element analysis; multibody kinematics, dynamics, and control; fabric mechanics; and stress analysis in microelectronic devices. Eischen received his BS in civil engineering from the University of California at Los Angeles. He did his MS and PhD graduate work in applied mechanics at Stanford University.*

Shigan Deng *works for the Aeronautical Research laboratory at Chung-Shan Institute of Technology, Taiwan. He received his BS in aeronautical engineering at TamKang University. He did MS and PhD graduate work in mechanical engineering at North Carolina State University.*

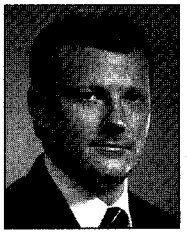

Timothy G. Clapp *is associate professor of textile engineering, chemistry, and science at North Carolina State University. His research interests include apparel automation and automated material handling. Clapp received his BS, MS, and PhD in mechanical engineering at North Carolina State University.*

Readers may contact Jeffrey Eischen at the Dept. of Mechanical and Aerospace Engineering, North Carolina State University, Box 7910, Raleigh, NC 27695-7910, e-mail eischen@eos.ncsu.edu.